Available online at www.sciencedirect.com
SCIENCE DIRECT
Journal of Sound and Vibration 286 (2005) 549–568
JOURNAL OF SOUND AND VIBRATION
www.elsevier.com/locate/jsvi

An exact solution for the natural frequencies and mode shapes of an immersed elastically restrained wedge beam carrying an eccentric tip mass with mass moment of inertia

Jong-Shyong Wu*, Chin-Tzu Chen

Department of Naval Architecture and Marine Engineering, National Cheng-Kung University, Tainan, Taiwan 701, Republic of China

Received 26 April 2004; received in revised form 27 August 2004; accepted 13 October 2004
Available online 28 December 2004

Abstract

In general, the exact solutions for natural frequencies and mode shapes of non-uniform beams are obtainable only for a few types such as wedge beams. However, the exact solution for the natural frequencies and mode shapes of an immersed wedge beam is not obtained yet. This is because, due to the "added mass" of water, the mass density of the immersed part of the beam is different from its emerged part. The objective of this paper is to present some information for this problem. First, the displacement functions for the immersed part and emerged part of the wedge beam are derived. Next, the force (and moment) equilibrium conditions and the deflection compatibility conditions for the two parts are imposed to establish a set of simultaneous equations with eight integration constants as the unknowns. Equating to zero the coefficient determinant one obtains the frequency equation, and solving the last equation one obtains the natural frequencies of the immersed wedge beam. From the last natural frequencies and the above-mentioned simultaneous equations, one may determine all the eight integration constants and, in turn, the corresponding mode shapes. All the analytical solutions are compared with the numerical ones obtained from the finite element method and good agreement is achieved. The formulation of this paper is available for the fully or partially immersed doubly tapered beams with square, rectangular or circular cross-sections. The taper ratio for width and that for depth may also be equal or unequal.

*Corresponding author. Fax: +886 6 280 8458.
E-mail address: jswu@mail.ncku.edu.tw (J.-S. Wu).

doi:10.1016/j.jsv.2004.10.008

1. Introduction

Since the dynamic behaviors of some structural systems, such as piles, water towers, fixed-type platforms, robot arms and tall buildings, can be predicted from a cantilever beam carrying a tip mass with reasonable accuracy, the literature concerned is plenty. For the uniform ‘‘*dry beam*’’ (without contacting with water or liquid) carrying a concentrated mass at its free end, the pertinent literature includes the works of Gürgöze [1,2], Laura, et al. [3], Posiadala [4], Rossi, et al. [5], Stephen [6], Takahashi [7], White and Heppler [8], and Wu and Lin [9]. For the non-uniform (particularly the linearly tapered) dry beam with tip mass, reports of Auciello [10], Goel [11], Laura and Gutierrez [12], Lee [13], Mabie and Rogers [14], Lau [15], and Wu and Chen [16] are the most concerned. Comparing with the ‘‘dry beams’’, the literature relating to the ‘‘wet beams’’ (fully or partially immersed in water) is relatively sparse. The few contributors are: Chang and Liu [17], Han and Sahglivi [18], Nagaya [19], Nagaya and Hai [20], Uscilowska and Kolodziej [21], and Wu and Chen [22]. It can be seen that most of the papers relating to the wet beams are to appear in the reference lists of Refs. [17,21,22]. By means of the transfer matrix method (TMM), Chang and Liu [17] studied the natural frequencies of the fully and partially immersed restrained columns. The structural models that they studied include the truncated solid and hollow cones, and the doubly tapered beams with various taper ratios and various magnitudes of tip masses and mass moment of inertias. By using the analytical method, Uscilowska and Kolodziej [21] studied the ‘‘exact’’ eigenfrequencies and eigenfunctions of a uniform cantilever column carrying a tip mass in the fully and partially immersed conditions. Using of the analytical-and-numerical-combined method, Wu and Chen [22] determined the lowest five approximate natural frequencies and mode shapes of the fully and partially immersed cantilever wedge beams carrying tip masses. From the existing literature [17,21], one finds that the technique used for the free vibration analysis of the wet beam is the same as that of the *dry beam*, the only difference is to replace the mass density of material for the dry beam, ρ, by $\rho + C'_m\tilde{\rho}$, where $\tilde{\rho}$ is the mass density of the water surrounding the beam and C'_m is the added mass coefficient relating to the shapes of the beam. It is evident that this kind of approach will suffer difficulty for the partially immersed column, because a cantilever beam with part of its length immersed in water is equivalent to a two-span beam, and achieving the analytical solution is very difficult, as shown by Uscilowska and Kolodziej [21]. In this paper, the same solution procedures as in Ref. [21] were used to determine the ‘‘exact’’ natural frequencies and the associated mode shapes for the fully or partially immersed restrained wedge beam carrying an eccentric tip mass possessing mass moment of inertia. Although the solution procedures of this paper are the same as those of Ref. [21], there exist some differences: (i) the beam studied in this paper is non-uniform and that in Ref. [21] is uniform; (ii) because of the last difference in the beam types, the displacement functions for the non-uniform (wedge) beam studied in this paper are in terms of the Bessel functions and those for the uniform beam in Ref. [21] are in terms of the transcendent functions; (iii) to model the interactions between the beam and the bottom soil, the lower (larger) end of the wedge beam is assumed to be restrained by a translation spring and a rotational spring in this paper, but the lower end of the uniform beam is assumed to be fixed in Ref. [21]. The formulation of this paper is available for the tapered beams with taper ratio of width being different from that of depth [23], but this is not true for some of the existing literature [10,12–14]. In addition to comparing with the existing information, all the numerical results of this paper were checked with the corresponding ones obtained from the conventional finite element method (FEM), and good agreement was achieved. The formulation of this paper is available for the tapered beams with either square or circular cross-sections. To save space, only the square tapered beams are studied in this paper. The influence of water depths and soil stiffness ratios on the free vibration characteristics of the fully or partially immersed doubly tapered beams is investigated.

2. Equations of motion and closed-form solutions for an immersed wedge beam

By neglecting the effects of shear deformation and rotary inertia, the equations of motion for the immersed tapered beam, as shown in Fig. 1, are given by [21,22,24]

$$\frac{\partial^2}{\partial x^2}\left[EI(x)\frac{\partial^2 y(x,t)}{\partial x^2}\right]+\rho A(x)\frac{\partial^2 y(x,t)}{\partial t^2}=0 \quad \text{for } L_0 \leqslant x \leqslant L_w, \tag{1a}$$

$$\frac{\partial^2}{\partial x^2}\left[EI(x)\frac{\partial^2 \tilde{y}(x,t)}{\partial x^2}\right]+(\rho + C'_m\tilde{\rho})A(x)\frac{\partial^2 \tilde{y}(x,t)}{\partial t^2}=0 \quad \text{for } L_w \leqslant x \leqslant L_{\mathrm{I}}, \tag{1b}$$

where E is Young's modulus, $A(x)$ is the cross-sectional area of the beam, $I(x)$ is the moment of inertia of$A(x)$, ρ is the mass density of beam material, $\tilde{\rho}$ is the mass density of water, C'_m is the added mass coefficient for $A(x)$ [25,26], $y(x,t)$ (or $\tilde{y}(x,t)$) is the transverse displacement at position x and time t. Besides, L_1, L_0 and L_w are the distances from the origin 0 of the xyz coordinate system to the larger end of the tapered beam, the smaller end of the tapered beam and the free

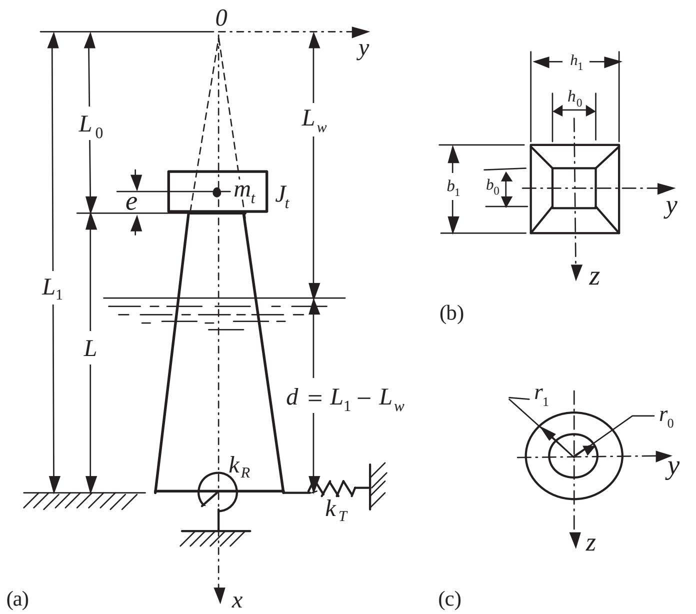

Fig. 1. Sketch for the immersed doubly tapered beam studied: (a) front view; (b) top view for the beam with rectangular cross-sections; (c) top view for the beam with circular cross-sections.

water surface, respectively. It is evident that L_1 denotes the length of the "complete" tapered beam, $L = L_1 - L_0$ denotes the length of the "truncated" tapered beam and $d = L_1 - L_w$ denotes the immersed length of the beam (or the water depth). It is noted that the origin 0 of the xyz coordinate system is located at the tip end of the complete tapered beam (see Fig. 1(a)).

For free vibration, one has

$$y(x,t) = W(x)\mathrm{e}^{\mathrm{i}\omega t} \quad \text{for } L_0 \leqslant x \leqslant L_w, \tag{2a}$$

$$\tilde{y}(x,t) = \tilde{W}(x)\mathrm{e}^{\mathrm{i}\omega t} \quad \text{for } L_w \leqslant x \leqslant L_1, \tag{2b}$$

where $W(x)$ and $\tilde{W}(x)$ denote the amplitude functions of $y(x,t)$ and $\tilde{y}(x,t)$, and represent the mode shapes of the emerged part and the immersed part of the partially immersed beam, respectively. In other words, any one mode shape of the entire partially immersed beam, $\bar{W}(x)$, is a combination of $W(x)$ and $\tilde{W}(x)$; thus, $\bar{W}(x) \equiv W(x)$ for a fully emerged beam (i.e.,$L_w = L_0$) and $\bar{W}(x) \equiv \tilde{W}(x)$ for a fully immersed beam (i.e.,$L_w = L_1$). Besides, in Eq. (2), ω is the natural frequency of the immersed beam, t is time and $\mathrm{i} = \sqrt{-1}$.

The substitution of Eqs. (2a) and (2b) into Eqs. (1a) and (1b), respectively, leads to

$$\frac{\mathrm{d}^2}{\mathrm{d}x^2}\left[EI(x)\frac{\mathrm{d}^2 W(x)}{\mathrm{d}x^2}\right] - \omega^2 \rho A(x) W(x) = 0 \quad \text{for } L_0 \leqslant x \leqslant L_w, \tag{3a}$$

$$\frac{\mathrm{d}^2}{\mathrm{d}x^2}\left[EI(x)\frac{\mathrm{d}^2 \tilde{W}(x)}{\mathrm{d}x^2}\right] - \omega^2 (\rho + C_m'\tilde{\rho}) A(x) \tilde{W}(x) = 0 \quad \text{for } L_w \leqslant x \leqslant L_1. \tag{3b}$$

For the linearly tapered beam with rectangular cross-sections, the area A_1 and the moment of inertia I_1 at its larger end (located at $x = L_1$) are given by

$$A_1 = b_1 h_1 \quad \text{and} \quad I_1 = b_1 h_1^3/12 \tag{4a,b}$$

and those for the arbitrary cross-section located at

$$\xi = x/L_1 \tag{5}$$

are given by

$$A(\xi) = A_1 \xi^2 \quad \text{and} \quad I(\xi) = I_1 \xi^4, \tag{6a,b}$$

where b_1 and h_1 are the width and depth of the cross-section at the larger end of the tapered beam (with $\xi = x/L_1 = 1$), respectively, as one may see from Fig. 1(b). Therefore, the solutions of Eqs. (3a) and (3b) take the forms [22,23,27]

$$W(\xi) = L_1^{-1}\xi^{-1}[c_1 J_2(z) + c_2 Y_2(z) + c_3 I_2(z) + c_4 K_2(z)] \quad \text{for } L_0 \leqslant x \leqslant L_w, \tag{7a}$$

$$\tilde{W}(\xi) = L_1^{-1}\xi^{-1}[\tilde{c}_1 J_2(\tilde{z}) + \tilde{c}_2 Y_2(\tilde{z}) + \tilde{c}_3 I_2(\tilde{z}) + \tilde{c}_4 K_2(\tilde{z})] \quad \text{for } L_w \leqslant x \leqslant L_1, \tag{7b}$$

where

$$z = 2\beta\xi^{1/2}, \quad \tilde{z} = 2\tilde{\beta}\xi^{1/2} \tag{8a,b}$$

with

$$\beta^4 = \omega^2 L_1^4\left(\frac{\rho A_1}{EI_1}\right), \quad \tilde{\beta}^4 = \omega^2 L_1^4\left[\frac{(\rho + C_m'\tilde{\rho})A_1}{EI_1}\right]. \tag{9a,b}$$

In Eqs. (7a) and (7b), J_2 and Y_2 are the second-order Bessel functions of first and second kind, respectively, I_2 and K_2 are the second-order modified Bessel functions of first and second kind, respectively, while c_i and $\tilde{c}_i$ $(i = 1{-}4)$ are the integration constants determined by the following boundary conditions:

$$EI(\xi)W''(\xi) = m_t e\omega^2 W(\xi) - (J_t + m_t e^2)\omega^2 W'(\xi) \quad \text{at } \xi = \xi_0 = L_0/L_1, \tag{10a}$$

$$\frac{\mathrm{d}}{L_1\mathrm{d}\xi}[EI(\xi)W''(\xi)] = m_t\omega^2 W(\xi) - m_t e\omega^2 W'(\xi) \quad \text{at } \xi = \xi_0 = L_0/L_1, \tag{10b}$$

$$W(\xi) = \tilde{W}(\xi), \quad W'(\xi) = \tilde{W}'(\xi), \quad W''(\xi) = \tilde{W}''(\xi), \quad W'''(\xi) = \tilde{W}'''(\xi)$$
$$\text{at } \xi = \xi_w = L_w/L_1, \tag{11a–d}$$

$$-EI(\xi)\tilde{W}''(\xi) = k_R\tilde{W}'(\xi) \quad \text{at } \xi = \xi_1 = L_1/L_1 = 1, \tag{12a}$$

$$\frac{\mathrm{d}}{L_1\mathrm{d}\xi}[EI(\xi)\tilde{W}''(\xi)] = k_T\tilde{W}(\xi) \quad \text{and} \quad \xi = \xi_1 = L_1/L_1 = 1, \tag{12b}$$

where

$$W'(\xi) = \mathrm{d}W(\xi)/\mathrm{d}\xi \quad \text{and} \quad \tilde{W}'(\xi) = \mathrm{d}\tilde{W}(\xi)/\mathrm{d}\xi.$$

Among the last eight equations, Eqs. (10a) and (10b) assure the equilibrium of bending moment and shear force at the top end of the tapered beam ((located at $\xi = \xi_0 = L_0/L_1$, as one may see from Fig. 1(a)), Eqs. (11a)–(11d) assure the compatibility of displacement and slope together with the moment equilibrium and force equilibrium at the junction of the emerged part and immersed part of the tapered beam (located at free water surface with $\xi = \xi_w = L_w/L_1$), while Eqs. (12a) and (12b) assure the equilibrium of bending moment and shear force at the lower end of the tapered beam (located at $\xi = \xi_1 = L_1/L_1 = 1.0$). It is noted that, in Eqs. (10a) and (10b), the symbols m_t and J_t denote the mass and mass moment of inertia for the lumped mass at the top end of the tapered beam (see Fig. 1(a)), respectively, and e denotes the eccentricity of the lumped mass m_t. Besides, the symbols k_R and k_T appearing in Eqs. (12a) and (12b) denote the spring constants for the rotational and translational (helical) springs at the lower end of the tapered beam, respectively, as one may see from Fig. 1(a).

Substituting Eq. (7a) into Eqs. (10a) and (10b), one obtains

$$B_{11}c_1 + B_{12}c_2 + B_{13}c_3 + B_{14}c_4 = 0, \tag{13a}$$

$$B_{21}c_1 + B_{22}c_2 + B_{23}c_3 + B_{24}c_4 = 0, \tag{13b}$$

where

$$\begin{aligned} B_{11} &= a_2J_2(z_0) + a_3J_3(z_0) - a_4J_4(z_0), \\ B_{12} &= a_2Y_2(z_0) + a_3Y_3(z_0) - a_4Y_4(z_0), \\ B_{13} &= a_2I_2(z_0) - a_3I_3(z_0) - a_4I_4(z_0), \\ B_{14} &= a_2K_2(z_0) + a_3K_3(z_0) - a_4K_4(z_0), \end{aligned} \tag{14a}$$

$$\begin{aligned} B_{21} &= b_2J_2(z_0) + b_3J_3(z_0) - b_4J_4(z_0) + b_5J_5(z_0), \\ B_{22} &= b_2Y_2(z_0) + b_3Y_3(z_0) - b_4Y_4(z_0) + b_5Y_5(z_0), \\ B_{23} &= b_2I_2(z_0) - b_3I_3(z_0) - b_4I_4(z_0) - b_5I_5(z_0), \\ B_{24} &= b_2K_2(z_0) + b_3K_3(z_0) - b_4K_4(z_0) + b_5K_5(z_0), \end{aligned} \tag{14b}$$

with

$$a_2 = m_te\omega^2L_1^{-2/2}\xi_0^{-2/2}, \quad a_3 = (J_t + m_te^2)\omega^2\beta L_1^{-4/2}\xi_0^{-3/2}, \quad a_4 = EI_0\beta^2L_1^{-6/2}\xi_0^{-4/2}, \tag{15}$$

$$\begin{aligned} &b_2 = m_t\omega^2L_1^{-2/2}\xi_0^{-2/2}, \quad b_3 = m_te\omega^2\beta L_1^{-4/2}\xi_0^{-3/2}, \\ &b_4 = EI_0'\beta^2L_1^{-6/2}\xi_0^{-4/2}, \quad b_5 = EI_0\beta^3L_1^{-8/2}\xi_0^{-5/2}, \end{aligned} \tag{16}$$

$$I_0 = I_1\xi_0^4, \tag{17}$$

$$I_0' = 4\xi_0^3I_1/L_1, \tag{18}$$

$$z_0 = 2\beta\xi_0^{1/2}. \tag{19}$$

Similarly, inserting Eqs. (7a) and (7b) into Eqs. (11a)–(11d) leads to

$$B_{31}c_1 + B_{32}c_2 + B_{33}c_3 + B_{34}c_4 + B_{35}\tilde{c}_1 + B_{36}\tilde{c}_2 + B_{37}\tilde{c}_3 + B_{38}\tilde{c}_4 = 0, \tag{20a}$$

$$B_{41}c_1 + B_{42}c_2 + B_{43}c_3 + B_{44}c_4 + B_{45}\tilde{c}_1 + B_{46}\tilde{c}_2 + B_{47}\tilde{c}_3 + B_{48}\tilde{c}_4 = 0, \tag{20b}$$

$$B_{51}c_1 + B_{52}c_2 + B_{53}c_3 + B_{54}c_4 + B_{55}\tilde{c}_1 + B_{56}\tilde{c}_2 + B_{57}\tilde{c}_3 + B_{58}\tilde{c}_4 = 0, \tag{20c}$$

$$B_{61}c_1 + B_{62}c_2 + B_{63}c_3 + B_{64}c_4 + B_{65}\tilde{c}_1 + B_{66}\tilde{c}_2 + B_{67}\tilde{c}_3 + B_{68}\tilde{c}_4 = 0, \tag{20d}$$

where

$$\begin{aligned} &B_{31} = J_2(z_w), \quad B_{32} = Y_2(z_w), \quad B_{33} = I_2(z_w), \quad B_{34} = K_2(z_w), \\ &B_{35} = -J_2(\tilde{z}_w), \quad B_{36} = -Y_2(\tilde{z}_w), \quad B_{37} = -I_2(\tilde{z}_w), \quad B_{38} = -K_2(\tilde{z}_w), \end{aligned} \tag{21a}$$

$$\begin{aligned} &B_{41} = \beta J_3(z_w), \quad B_{42} = \beta Y_3(z_w), \quad B_{43} = -\beta I_3(z_w), \quad B_{44} = \beta K_3(z_w), \\ &B_{45} = -\tilde{\beta}J_3(\tilde{z}_w), \quad B_{46} = -\tilde{\beta}Y_3(\tilde{z}_w), \quad B_{47} = \tilde{\beta}I_3(\tilde{z}_w), \quad B_{48} = -\tilde{\beta}K_3(\tilde{z}_w), \end{aligned} \tag{21b}$$

$$B_{51} = \beta^2 J_4(z_w), \quad B_{52} = \beta^2 Y_4(z_w), \quad B_{53} = \beta^2 I_4(z_w), \quad B_{54} = \beta^2 K_4(z_w),$$
$$B_{55} = -\tilde{\beta}^2 J_4(\tilde{z}_w), \quad B_{56} = -\tilde{\beta}^2 Y_4(\tilde{z}_w), \quad B_{57} = -\tilde{\beta}^2 I_4(\tilde{z}_w), \quad B_{58} = -\tilde{\beta}^2 K_4(\tilde{z}_w), \tag{21c}$$

$$B_{61} = \beta^3 J_5(z_w), \quad B_{62} = \beta^3 Y_5(z_w), \quad B_{63} = -\beta^3 I_5(z_w), \quad B_{64} = \beta^3 K_5(z_w),$$
$$B_{65} = -\tilde{\beta}^3 J_5(\tilde{z}_w), \quad B_{66} = -\tilde{\beta}^3 Y_5(\tilde{z}_w), \quad B_{67} = \tilde{\beta}^3 I_5(\tilde{z}_w), \quad B_{68} = -\tilde{\beta}^3 K_5(\tilde{z}_w), \tag{21d}$$

with

$$z_w = 2\beta\xi_w^{1/2}, \tag{22}$$

$$\tilde{z}_w = 2\tilde{\beta}\xi_w^{1/2}. \tag{23}$$

When Eq. (7b) is substituted into the two boundary equations given by Eqs. (12a) and (12b), one obtains

$$B_{75}\tilde{c}_1 + B_{76}\tilde{c}_2 + B_{77}\tilde{c}_2 + B_{78}\tilde{c}_4 = 0, \tag{24}$$

$$B_{85}\tilde{c}_1 + B_{86}\tilde{c}_2 + B_{87}\tilde{c}_3 + B_{88}\tilde{c}_4 = 0, \tag{25}$$

where

$$B_{75} = d_3 J_3(\tilde{z}_1) - d_4 J_4(\tilde{z}_1), \quad B_{76} = d_3 Y_3(\tilde{z}_1) - d_4 Y_4(\tilde{z}_1),$$
$$B_{77} = -d_3 I_3(\tilde{z}_1) - d_4 I_4(\tilde{z}_1), \quad B_{78} = d_3 K_3(\tilde{z}_1) - d_4 K_4(\tilde{z}_1), \tag{26a}$$

$$B_{85} = e_2 J_2(\tilde{z}_1) - e_4 J_4(\tilde{z}_1) + e_5 J_5(\tilde{z}_1), \quad B_{86} = e_2 Y_2(\tilde{z}_1) - e_4 Y_4(\tilde{z}_1) + e_5 Y_5(\tilde{z}_1),$$
$$B_{87} = e_2 I_2(\tilde{z}_1) - e_4 I_4(\tilde{z}_1) - e_5 I_5(\tilde{z}_1), \quad B_{88} = e_2 K_2(\tilde{z}_1) - e_4 K_4(\tilde{z}_1) + e_5 K_5(\tilde{z}_1), \tag{26b}$$

with

$$d_3 = k_R\tilde{\beta}L_1^{-4/2}\xi_1^{-3/2}, \quad d_4 = EI_1\tilde{\beta}^2 L_1^{-6/2}\xi_1^{-4/2}, \tag{27}$$

$$e_2 = k_T L_1^{-2/2}\xi_1^{-2/2}, \quad e_4 = EI_1'\tilde{\beta}^2 L_1^{-6/2}\xi_1^{-4/2}, \quad e_5 = EI_1\tilde{\beta}^3 L_1^{-8/2}\xi_1^{-5/2}, \tag{28}$$

$$\tilde{z}_1 = 2\tilde{\beta}\xi_1^{1/2} = 2\tilde{\beta}, \tag{29}$$

$$I_1' = 4I_1/L_1. \tag{30}$$

The foregoing eight equations, (13a), (13b), (20a)–(20d), (25a) and (25b), constitute a set of simultaneous equations for the eight integration constants, c_i and $\tilde{c}_i$ $(i = 1-4)$. Non-trivial solution for the last simultaneous equations requires that their coefficient determinant is equal to zero, i.e.,

$$\Delta(\omega) = \begin{vmatrix} B_{11} & B_{12} & B_{13} & B_{14} & 0 & 0 & 0 & 0 \\ B_{21} & B_{22} & B_{23} & B_{24} & 0 & 0 & 0 & 0 \\ B_{31} & B_{32} & B_{33} & B_{34} & B_{35} & B_{36} & B_{37} & B_{38} \\ B_{41} & B_{42} & B_{43} & B_{44} & B_{45} & B_{46} & B_{47} & B_{48} \\ B_{51} & B_{52} & B_{53} & B_{54} & B_{55} & B_{56} & B_{57} & B_{58} \\ B_{61} & B_{62} & B_{63} & B_{64} & B_{65} & B_{66} & B_{67} & B_{68} \\ 0 & 0 & 0 & 0 & B_{75} & B_{76} & B_{77} & B_{78} \\ 0 & 0 & 0 & 0 & B_{85} & B_{86} & B_{87} & B_{88} \end{vmatrix} = 0. \tag{31}$$

If the lower (larger) end of the tapered beam is clamped (or fixed), the boundary conditions given by Eqs. (12a) and (12b) must be replaced by (cf. Fig. 1(a))

$$\tilde{W}(\xi) = \frac{\mathrm{d}\tilde{W}(\xi)}{L_1 \mathrm{d}\xi} = 0 \quad \text{at} \;\; \xi = \xi_1 = 1. \tag{32a,b}$$

In such a case, all the foregoing formulations are valid if the coefficients B_{7i} and B_{8i} ($i = 5{-}8$) appearing in Eqs. (25), (26) and (31) are replaced by

$$\begin{aligned} &B_{75} = J_2(\tilde{z}_1), \quad B_{76} = Y_2(\tilde{z}_1), \quad B_{77} = I_2(\tilde{z}_1), \quad B_{78} = K_2(\tilde{z}_1), \\ &B_{85} = J_3(\tilde{z}_1), \quad B_{86} = Y_3(\tilde{z}_1), \quad B_{87} = -I_3(\tilde{z}_1), \quad B_{88} = K_3(\tilde{z}_1). \end{aligned} \tag{33}$$

Eq. (31) is the frequency equation and is solved for the natural frequencies ω_r ($r = 1, 2, \ldots$) of the immersed tapered beam by using the half-interval method [28] in this paper. Corresponding to each natural frequency ω_r, one may obtain a set of integration constants, c_i and $\tilde{c}_i$ ($i = 1{-}4$), from the above-mentioned simultaneous equations. Substituting these constants into Eqs. (7a) and (7b) will determine the associated rth emerged-part and immersed-part mode shapes, $W^{(r)}(\xi)$ and $\tilde{W}^{(r)}(\xi)$, respectively. The combination of $W^{(r)}(\xi)$ and $\tilde{W}^{(r)}(\xi)$ gives the rth mode shape of the entire immersed tapered beam.

If the taper ratios for the variations of width and depth of the beam are defined by (see Figs. 1(a) and (b))

$$\alpha_b = b_1/L_1 = b_0/L_0 \quad \text{and} \quad \alpha_h = h_1/L_1 = h_0/L_0, \tag{34a,b}$$

then, for a complete tapered beam with length L_1, the taper ratios α_b and α_h (or the maximum width b_1 and maximum depth h_1) may take any values and Eqs. (6) and (7) are always satisfied. In other words, the formulation of this paper is available for the doubly tapered beams with the square, rectangular or circular cross-sections. For example, if the cross-sections of the doubly tapered beam are circular with diameter d_1 at the larger end (see Fig. 1(c)), then one only requires to replace the values of A_1 and I_1 given by Eqs. (4a) and (4b) by the following ones; the foregoing formulations are still available:

$$A_1 = \pi d_1^2/4 \text{ and } I_1 = \pi d_1^2/64. \tag{35a,b}$$

In Ref. [10], the taper ratios for the width and depth of a tapered beam are defined by b_1/b_0 and h_1/h_0, respectively. It is believed that the more significant definitions for the taper ratios should be the ratios between the characteristic length for the transverse dimension and that for the longitudinal (or axial) dimension, such as those given by Eq. (34), rather than the ratios between the transverse dimensions of a tapered beam only.

3. The finite element model for the immersed wedge beam

To confirm the reliability of the above formulations, the exact values of natural frequencies and the corresponding mode shapes are checked by the numerical results obtained from the conventional FEM. The mathematical model for the FEM is shown in Fig. 2, where the whole tapered beam is replaced by an equivalent stepped beam composed of N_e uniform beam elements bounded by $N_e + 1$ nodes. Besides, the added mass for the immersed part of the wedge beam is also replaced by a number of point masses, as shown by the symbol ● appearing in Fig. 2. The last point added masses are attached to the nodes of the associated uniform beam elements. For the details about the calculation of point added masses, one may refer to Ref. [22].

4. Numerical results and discussions

The formulation of this paper is available for the tapered beams with either square or circular cross-sections. Because the dynamic behaviours of the square tapered beams are similar to those of the circular ones, only the square tapered beams are studied in this section. Except the first

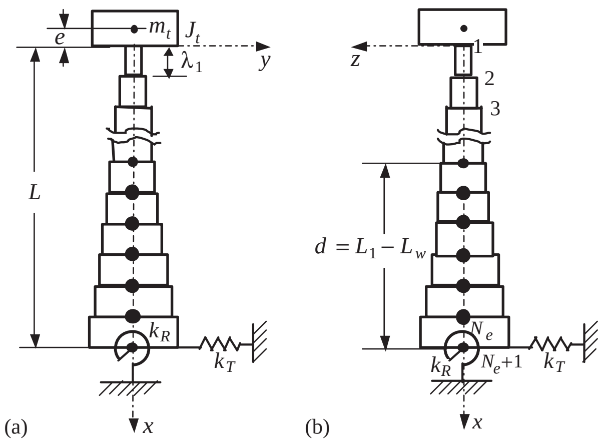

Fig. 2. The discrete finite element model for the immersed wedge beam: (a) front view and (b) right side view. (The digits in (b) denote the node numberings.)

example for comparing with the existing literature [10], the dimensions for all the square tapered beams are as follows (cf. Fig. 1): distance from origin 0 to the larger end is $L_1 = 33$ m, that to the smaller end is $L_0 = 11$ m, the width and depth for the cross-section at the larger end are $b_1 = L_1 = 3.3$ m, those at the smaller end are $b_0 = L_0 = 1.1$ m. According to the definitions of this paper given by Eq. (34), one has the taper ratios $\alpha_b = \alpha_h = h_1/L_1 = h_0/L_0 = 0.1$. The physical properties of the beam material are: Young's modulus $E = 2.068 \times 10^{11}$ N/m^2 and mass density $\rho = 7850$ kg/m^3. For convenience, the added mass coefficient is assumed to be $C'_m = 1.0$.

4.1. Reliability of the theory and the computer programs (for water depth $d = 0$)

In order to compare the results of this paper with those of Ref. [10], the dimensions of the square tapered beam for the present first example are selected the same as those for the other examples, except that the distance from origin 0 to the smaller end is $L_0 = 30$ m instead of $L_0 = 11$ m. In such a case, the width and depth for the cross-section at the smaller end are given by $b_0 = h_0 = 3.0$ m. Therefore, according to the definition in Ref. [10], the ratio of $h_1/h_0 = 3.3/3 = 1.1$ is equal to the taper ratios for the tapered beam of Table 4 in Ref. [10]. From the foregoing given data for the present example 1, one obtains: cross-sectional area of the larger end $A_1 = b_1 h_1 = 10.89$ m^2, that of the smaller end $A_0 = b_0 h_0 = 9$ m^2, moment of inertia for the cross-sectional area at the larger end $I_1 = b_1 h_1^3/12 = 9.882675$ m^4, that at the smaller end $I_0 = b_0 h_0^3/12 = 6.75$ m^4, the total mass of the tapered beam $m_b = \rho(A_1 L_1 - A_0 L_0)/3 = 2.338515 \times 10^5$ kg, and the total length of the "truncated" wedge beam $L = L_1 - L_0 = 3$ m. Based on the above physical quantities, the spring constant of the translational (helical) spring $k_T = (EI_1/L^3)/C_T = 7.569397 \times 10^{10}/C_T$ and that of the rotational spring $k_R = (EI_1/L)/C_R = 6.8124573 \times 10^{11}/C_R$ to agree with the "conditions" given by Table 4 of Ref. [10] are listed in Table 1, where C_T and C_R are the soil stiffness ratios defined by $C_T = EI_1/(k_T L^3)$ and $C_R = EI_1/(k_R L)$, respectively [10].

For the case of magnitude of lumped mass $m_t = m_b = 2.338515 \times 10^5$ kg and mass moment of inertia $J_t = m_t\,(0.6L)^2 = 7.5767886 \times 10^5$ kg m^2 with eccentricity $e = 0.4L = 1.2$ m, together with

Table 1
The magnitudes of spring constants of k_T and k_R for the combinations of $C_T = EI_1/(k_T L^3)$ and $C_R = EI_1/(k_R L)$ being equal to 0.0, 0.1, 1.0 and 10.0

C_T	C_R	k_T (N/m)	k_R (N m)
0 (fixed supported)	0.1	∞	6.8124573×10^{12}
	1.0		6.8124573×10^{11}
	10		6.8124573×10^{10}
0.1 (elastically supported)	0.1	7.569397×10^{11}	6.8124573×10^{12}
	1.0		6.8124573×10^{11}
	10		6.8124573×10^{10}
1.0 (elastically supported)	0.1	7.569397×10^{10}	6.8124573×10^{12}
	1.0		6.8124573×10^{11}
	10		6.8124573×10^{10}

Note: $k_T = 7.569397 \times 10^{10}/C_T$ N/m, $k_R = 6.8124573 \times 10^{11}/C_R$ N m.

Table 2
The lowest five frequency coefficients $\bar{\beta}_r = \sqrt[4]{\omega_r^2 L^4 \rho A_0/(EI_0)}$ obtained from the present paper and Ref. [10] with $e = 0.4L$, $h_1/h_0 = 1.1$, $m_t = m_b$, $J_t = m_t(0.6L)^2$, $k_T = 7.569397 \times 10^{10}/C_T$ N/m, $k_R = 6.8124573 \times 10^{11}/C_R$ N m and water depth $d = 0$

C_T	C_R	Methods	Frequency coefficients, $\bar{\beta}_r = \sqrt[4]{\omega_r^2 L^4 \rho A_0/(EI_0)}$				
			$\bar{\beta}_1$	$\bar{\beta}_2$	$\bar{\beta}_3$	$\bar{\beta}_4$	$\bar{\beta}_5$
0.0	0.0	FEM	0.97201	2.28952	5.13362	8.22043	11.38786
		[a]Approximate	0.97201	2.28952	5.13507	8.23629	11.43806
		Exact	0.97201	2.28951	5.13362	8.22043	11.38786
		Ref. [10]	0.97201	2.28951	5.13362	—	—
	0.1	FEM	0.93456	2.18259	4.83462	7.81147	10.90524
		Approximate	0.93456	2.18258	4.83504	7.81497	10.91325
		Ref. [10]	0.93456	2.18258	4.83459	—	—
	1.0	FEM	0.75524	1.94887	4.45433	7.48491	10.62827
		Approximate	0.75524	1.94886	4.45430	7.48491	10.62828
		Ref. [10]	0.75524	1.94886	4.45428	—	—
	10	FEM	0.46743	1.85437	4.35816	7.42446	10.58453
		Approximate	0.46743	1.85436	4.35811	7.42436	10.58438
		Ref. [10]	0.46743	1.85436	4.35811	—	—
0.1	0.1	FEM	0.92059	1.76180	3.11806	5.69952	8.71937
		Exact	0.92059	1.76179	3.11803	5.69905	8.71564
		Ref. [10]	0.92060	1.76179	3.11803	—	—
	1.0	FEM	0.74960	1.71407	3.01056	5.30878	8.32336
		Exact	0.74961	1.71407	3.01054	5.30851	8.32185
		Ref. [10]	0.74961	1.71407	3.01053	—	—
	10	FEM	0.46688	1.68719	2.95723	5.16726	8.22105
		Exact	0.46688	1.68718	2.95721	5.16718	8.22097
		Ref. [10]	0.46688	1.68718	2.95720	—	—
1.0	0.1	FEM	0.80146	1.23842	2.89130	5.66064	8.70733
		Exact	0.80146	1.23842	2.89127	5.66021	8.70367
		Ref. [10]	0.80146	1.23842	2.89127	—	—
	1.0	FEM	0.70085	1.19769	2.63422	5.23965	8.30528
		Exact	0.70085	1.19769	2.63419	5.23937	8.30378
		Ref. [10]	0.70085	1.19769	2.63419	—	—
	10	FEM	0.46189	1.16527	2.48055	5.08750	8.20185
		Exact	0.46189	1.16527	2.48052	5.08740	8.20175
		Ref. [10]	0.46189	1.16527	2.48052	—	—

[a]The "approximate" values are based on the elastically supported beam with $C_T = C_R = 10^{-15}$(or $k_T = 7.569397 \times 10^{25}$ N/m and $k_R = 6.8124573 \times 10^{26}$ N m).

the various combinations of the spring constants of k_T and k_R shown in Table 1, the lowest five natural frequency coefficients, $\bar{\beta}_r = \sqrt[4]{\omega_r^2 L^4 \rho A_0/(EI_0)}$ are listed in Table 2 in which the "exact" values refer to the analytical solutions based on the formulations of this paper and the "FEM" values refer to the finite element solutions based on the mathematical model shown in Fig. 2 with the total number of beam elements $N_e = 50$. From Table 2, one sees that the exact values of this paper are equal to the corresponding ones of Ref. [10] exactly with very few exceptions, and the

FEM results are also very close to the corresponding exact ones. Therefore, both the analytical theory and the FEM computer programs presented for this paper should be reliable.

In Ref. [10], the stiffness ratios $C_T = EI_1/(k_T L^3) = 0$ and $C_R = EI_1/(k_R L) = 0$ refer to the supported condition that the lower end of the wedge beam is clamped (or fixed). To study the possibility of obtaining the natural frequencies of a wedge with its lower end fixed supported from the presented closed-form solutions based on the same wedge beam with its lower end elastically supported, we set $C_T = C_R = 10^{-15}$ (or $k_T = 7.569397 \times 10^{25}\,\mathrm{N/m}$ and $k_R = 6.8124573 \times 10^{26}\,\mathrm{N\,m}$) for the elastically supported beam and obtained the "approximate" values as shown in lines 4, 8, 11 and 14 of Table 2. It is evident that all the values of $\bar{\beta}_r$ $(r = 1-5)$, based on $C_T = C_R = 10^{-15}$, obtained either from FEM results or the "approximate" results, are very close to the "exact" values of the wedge beam with its lower end fixed (i.e., based on $C_T = C_R = 0$).

It is noted that: (i) most of the symbols in this paper are different from those in Ref. [10], e.g., the symbols A_0, I_0, A_1 and I_1 in this paper are corresponding to A_1, I_1, A_2 and I_2 in Ref. [10], respectively; (ii) the definitions for the taper ratio of width, α_b, and that of depth, α_h, in this paper are also different from those of Ref. [10]; (iii) most of the parameters are "dimensional" in this paper, but all parameters in Ref. [10] are "non-dimensional"; (iv) the formulation of this paper is available for the cases of $\alpha_b = \alpha_h$ and $\alpha_b \neq \alpha_h$, but this is true only for the case of $\alpha_b = \alpha_h$ in Ref. [10]. It is believed that carefully reading both this paper and Ref. [10] will be helpful for the readers to understand the statements of this subsection.

4.2. Influence of water depth on the natural frequencies of a fixed supported tower

In order to satisfy the "conditions" of Table 4 in Ref. [10], the length of the truncated wedge beam studied in the above example 1 is selected to be $L = 3\,\mathrm{m}$; however, this is too short for a practical off-shore tower. Therefore, the length of the wedge beam in the subsequent subsections is assumed to be $L = 22\,\mathrm{m}$, which is obtained from the above complete wedge beam with one-third of its total length at the smaller end being truncated. In other words, the dimensions for the current "truncated" wedge beam are those having been mentioned at the beginning of this section: $b_0 = h_0 = 1.1\,\mathrm{m}$, $b_1 = h_1 = 3.3\,\mathrm{m}$, $A_0 = b_0 h_0 = 1.21\,\mathrm{m}^2$, $A_1 = b_1 h_1 = 10.89\,\mathrm{m}^2$, $L_0 = 11\,\mathrm{m}$, and $L_1 = 33\,\mathrm{m}$. Thus, for this wedge beam, one has its length $L = L_1 - L_0 = 22\,\mathrm{m}$, its total mass $m_b = \rho(A_1 L_1 - A_0 L_0)/3 = 9.05523667 \times 10^5\,\mathrm{kg}$ and its taper ratios $\alpha_b = \alpha_h = h_1/L_1 = h_0/L_0 = 0.1$. It is evident that, for the current wedge beam, the ratio of h_1/h_0 $(= b_1/b_0)$ is equal to 3 rather than 1.1 for the wedge beam of Ref. [10].

The influence of water depths ($d = L_1 - L_w = 22$, 20, 15, 10, 5 and 0 m) on the lowest five natural frequencies of the last wedge beam with its lower (larger) end "fixed supported", i.e., with stiffness ratios $C_T = C_R = 0$, is shown in Table 3, in which the magnitude of tip mass (m_t) and its mass moment of inertia (J_t) along with its eccentricity (e) are assumed to be: $m_t = m_b = 9.05523667 \times 10^{-5}\,\mathrm{kg}$, $J_t = m_t\,(0.05L)^2 = 1.09568364 \times 10^6\,\mathrm{kg\,m}^2$ and $e = 0.05L = 1.1\,\mathrm{m}$. From Table 3, one finds that: (i) the natural frequency of the tower decreases with increasing the water depth (d) due to its added mass to increase with the increase in its immersion; (ii) the influence of water depth on the $(r+1)$th natural frequency ω_{r+1} is larger than that on the rth one ω_r $(r = 1-5)$ as one may see from Fig. 3, too; (iii) all the lowest five natural frequencies obtained from the FEM, $\omega_{r,\mathrm{FEM}}$, are very close to the corresponding exact ones, $\omega_{r,\mathrm{exact}}$, with the trend that

Table 3
Influence of water depths (d) on the lowest five natural frequencies of the "fixed supported" tower with $e = 0.05\,L = 1.1\,\mathrm{m}$, $m_t = m_b = 9.05523667 \times 10^5\,\mathrm{kg}$, and $J_t = m_t(0.05L)^2 = 1.09568364 \times 10^6\,\mathrm{kg\,m^2}$

Water depths d (m)	Methods	Natural frequencies, ω_r (rad/s)				
		ω_1	ω_2	ω_3	ω_4	ω_5
22	Exact	12.4457	84.8899	185.0669	395.0587	737.8604
	FEM	12.4452	84.8902	185.0964	395.1019	737.9203
20	Exact	12.4567	85.0232	185.3632	395.1301	738.5435
	FEM	12.4562	85.0234	185.3924	395.1741	738.6071
15	Exact	12.4738	86.3455	185.7314	403.1445	753.1635
	FEM	12.4732	86.3456	185.7614	403.1805	753.2254
10	Exact	12.4794	87.6808	188.8452	406.0575	765.2312
	FEM	12.4788	87.6814	188.8737	406.1017	765.2858
5	Exact	12.4803	88.0644	191.3257	414.7813	774.5528
	FEM	12.4797	88.0655	191.3559	414.8214	774.6075
0	Exact	12.4803	88.0823	191.5053	416.4709	781.4470
	FEM	12.4798	88.0834	191.5361	416.5149	781.5096

$\omega_{r,\mathrm{FEM}} > \omega_{r,\mathrm{exact}}$ for $r = 2\text{–}4$ and $\omega_{1,\mathrm{FEM}} < \omega_{1,\mathrm{exact}}$. The total number of beam elements for the FEM throughout this paper is $N_e = 110$, except in the last subsection (with $N_e = 50$).

It is noted that one of the main differences between the mathematical model for the exact method (cf. Fig. 1) and that for the FEM (cf. Fig. 2) is that the added mass for the former is distributed, but the last added mass is replaced by a number of concentrated masses for the latter. For this reason, the magnitude of each concentrated (lumped) mass and its relative position to the adjacent node for a specified mode shape will affect the associated approximate natural frequency and this is not true for the exact one. For example, for a beam carrying a number of point (added) masses, if the ith point mass is coincident with one of the nodes of the rth mode shape, then the contribution of the ith point mass on the rth natural frequency $\omega_{r,\mathrm{FEM}}$ is nil. However, this is not true for the corresponding exact value $\omega_{r,\mathrm{exact}}$. In other words, in addition to the total number of beam elements (N_e) for FEM, the approximate natural frequencies $\omega_{r,\mathrm{FEM}}$ are also dependent upon the water depth (d) and the supporting conditions at the lower (larger) end of the wedge tower (reflected by the soil stiffness ratios C_T and C_R). The last phenomenon will be the reason why the trend for the difference between the approximate frequencies $\omega_{r,\mathrm{FEM}}$ and their corresponding exact ones $\omega_{r,\mathrm{exact}}$, i.e., $\omega_{r,\mathrm{FEM}} - \omega_{r,\mathrm{exact}}$ ($r = 1 - 5$), for one specified case of water depth and supporting condition, is slightly different from that for the other case, as one may see from Table 4.

4.3. *Influence of water depths on the natural frequencies of an elastically supported tower*

For convenience, one assumes that the lower (larger) end of the off-shore tower is fixed, i.e., the soil stiffness ratios $C_T = C_R = 0$ or the spring constants $k_T = k_R = \infty$. It is obvious that the last

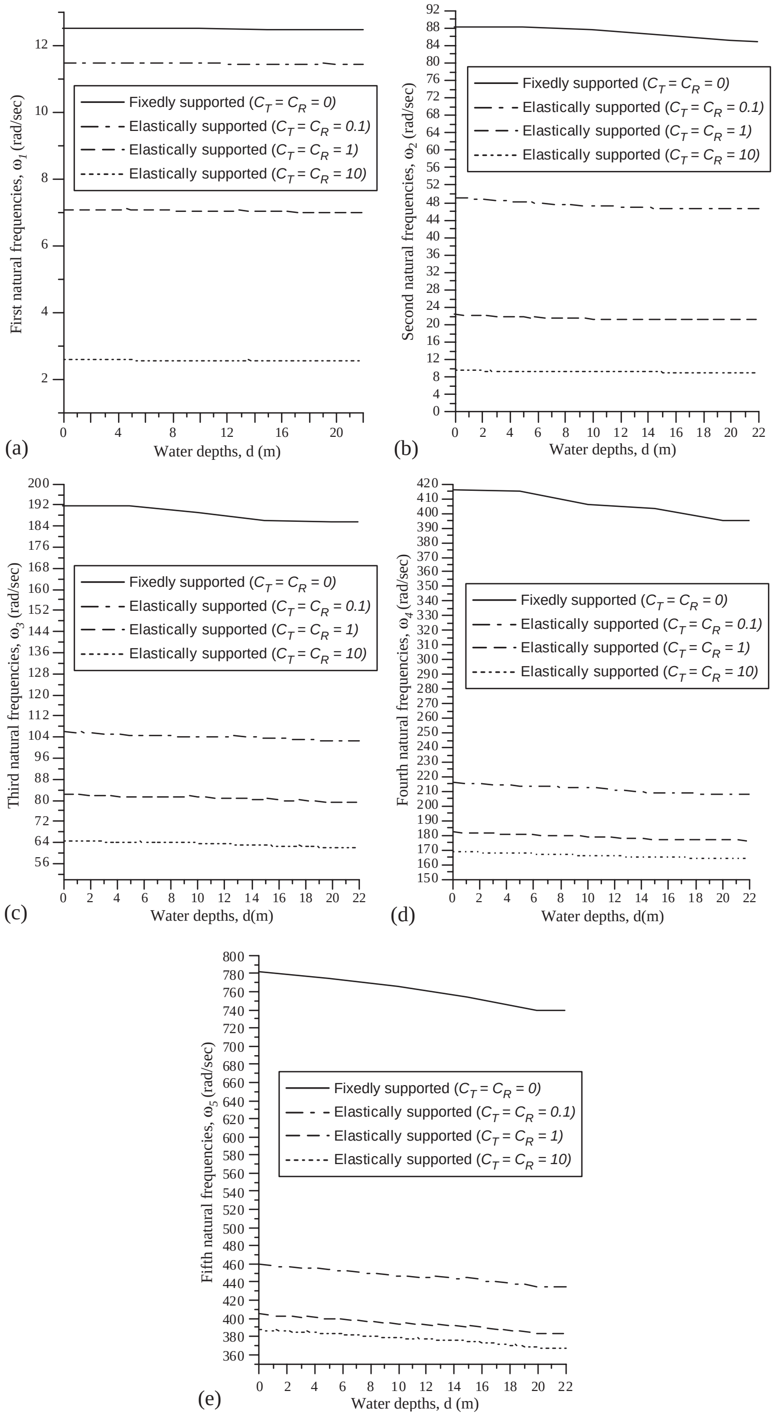

Fig. 3. Influence of water depths (d) on the lowest five natural frequencies of the tower with $C_T = C_R = 0$ (———), $C_T = C_R = 0.1$ (—·—·), $C_T = C_R = 1$ (– – – –) and $C_T = C_R = 10$ (······) for: (a) first natural frequencies ω_1, (b) second ones ω_2, (c) third ones ω_3, (d) fourth ones ω_4, and (e) fifth ones ω_5.

Table 4
Influence of soil stiffness (k_T and k_R) and water depths (d) on the lowest five natural frequencies of the "elastically supported" tower with $e = 0.05L = 1.1$ m, $m_t = m_b = 9.05523667 \times 10^5$ kg, $J_t = m_t(0.05L)^2 = 1.09568364 \times 10^6$ kg m^2, $k_T = 1.9193625 \times 10^8/C_T$ N/m and $k_R = 9.2897145 \times 10^{10}/C_R$ N m

Soil stiffness ratios $C_T = C_R$	Water depths d (m)	Methods	Natural frequencies, ω_r (rad/s)				
			ω_1	ω_2	ω_3	ω_4	ω_5
0.1	22	Exact	11.4201	46.5066	102.3399	207.9419	434.1806
		FEM	11.4197	46.5064	102.3459	207.9786	434.2363
	20	Exact	11.4308	46.5136	102.5263	208.1897	434.2647
		FEM	11.4303	46.5134	102.5322	208.2261	434.3214
	15	Exact	11.4504	46.6960	103.7383	208.8647	443.5467
		FEM	11.4500	46.6958	103.7443	208.9012	443.5953
	10	Exact	11.4605	47.2215	104.2048	212.6433	446.5189
		FEM	11.4601	47.2213	104.2116	212.6789	446.5753
	5	Exact	11.4650	48.0486	104.4197	213.5970	453.7144
		FEM	11.4646	48.0483	104.4266	213.6347	453.7694
	0	Exact	11.4672	49.1200	105.9650	216.1269	458.2526
		FEM	11.4668	49.1198	105.9723	216.1649	458.3117
1.0	22	Exact	6.9926	21.2598	79.1488	176.4985	383.1250
		FEM	6.9926	21.2597	79.1500	176.5313	383.1786
	20	Exact	6.9995	21.2603	79.2444	176.8203	383.1962
		FEM	6.9994	21.2602	79.2456	176.8527	383.2505
	15	Exact	7.0196	21.2761	80.2501	177.1460	390.9217
		FEM	7.0195	21.2760	80.2511	177.1796	390.9688
	10	Exact	7.0419	21.3871	81.1597	179.2018	393.9402
		FEM	7.0418	21.3870	81.1611	179.2345	393.9953
	5	Exact	7.0647	21.6949	81.2716	180.5633	399.8270
		FEM	7.0646	21.6948	81.2733	180.5973	399.8790
	0	Exact	7.0867	22.3240	82.4200	182.1954	403.6957
		FEM	7.0866	22.3239	82.4221	182.2311	403.7562
10	22	Exact	2.5264	9.1364	62.0460	164.2166	367.5604
		FEM	2.5265	9.1365	62.0450	164.2473	367.6134
	20	Exact	2.5288	9.1377	62.0925	164.5731	367.6344
		FEM	2.5288	9.1378	62.0916	164.6035	367.6880
	15	Exact	2.5372	9.1385	62.8047	164.9821	374.9347
		FEM	2.5373	9.1387	62.8036	165.0137	374.9814
	10	Exact	2.5488	9.1568	63.7514	166.3235	378.2305
		FEM	2.5488	9.1569	63.7504	166.3545	378.2849
	5	Exact	2.5625	9.2536	63.9723	167.6966	383.4887
		FEM	2.5626	9.2537	63.9715	167.7285	383.5400
	0	Exact	2.5771	9.5608	64.7297	168.8512	386.9874
		FEM	2.5772	9.5609	64.7294	168.8851	387.0478

assumption may be different from the actual situation to some degree. For this reason, this paper uses the translational (helical) spring constant k_T to model the sliding stiffness and the rotational spring constant k_R to model the rocking stiffness between the tower and the seabed. If the physical properties for the tip mass and the supporting springs are assumed to be $m_t = m_b = 9.05523667 \times 10^5$ kg, $J_t = m_t\,(0.05L)^2 = 1.09568364 \times 10^6$ kg m^2, $e = 0.05L = 1.1$ m, $k_T = 1.9193625 \times 10^8/C_T$ N/m and $k_R = 9.2897145\times 10^{10}/C_R$ N m, then the influence of soil stiffness ratios ($C_T = EI_1/(k_T L^3)$ and $C_R = EI_1/(k_R L)$) and water depths (d) on the lowest five natural frequencies of the "elastically supported" tower is shown in Table 4, where the soil stiffness ratios are $C_T = C_R = 0.1$, 1.0 and 10.0, while the water depths are $d = L_1 - L_w = 22$, 20, 15, 10, 5 and 0 m. It is noted that water depth $d = 0$ means the tower being on land and is called the "dry" tower, while $d \neq 0$ means the tower being partially or fully immersed in water and is called the "wet" tower in this paper. From Table 4, one sees that all conclusions drawn from the last subsection for Table 3 are available for Table 4. It is reasonable that all the natural frequencies shown in Table 4 are smaller than the corresponding ones shown in Table 3 and the lowest five natural frequencies of the elastically supported tower decrease with increasing the soil stiffness ratios (C_T and C_R) or decreasing the spring constants (k_T and k_R).

For clearness, the influence of water depths (d) and soil stiffness ratios (C_T and C_R) on the lowest five natural frequencies of the tower shown in Tables 3 and 4 is further plotted in Fig. 3, where the curves, ———, —·—·—, – – – – and ······, represent the cases of $C_T = C_R = 0$, $C_T = C_R = 0.1$, $C_T = C_R = 1$ and $C_T = C_R = 10$, respectively, and Figs. 3(a)–(e) are for the first natural frequencies (ω_1), second ones (ω_2), third ones (ω_3), fourth ones (ω_4) and fifth ones (ω_5), respectively. From Fig. 3, one sees that the influence of water depths on the first natural frequencies is negligible no matter whether $C_T = C_R = 0, 0.1$, 1.0 or 10, particularly for the fixed supported tower (with $C_T = C_R = 0$). However, the last phenomenon is not true for the other natural frequencies ω_r ($r = 2-5$). It is also found that the natural frequencies for the fixed supported tower (with $C_T = C_R = 0$) and the corresponding ones for the elastically supported tower with $C_T = C_R = 0.1$ are close to each other for the first mode ω_1 and are much divergent for the other modes ω_r ($r = 2-5$).

4.4. The lowest five mode shapes of the fixed and elastically supported towers

The lowest five mode shapes corresponding to some of the lowest five natural frequencies shown in Tables 3 and 4 are shown in Figs. 4 and 5, among which Fig. 4 shows the lowest five mode shapes of the fully immersed tower ($d = L = 22$ m) obtained from exact solutions (represented by the solid curves ———) and those from the FEM (represented by the dashed curves – – – –), with Fig. 4(a) for the fixed supported tower ($C_T = C_R = 0$) and Fig. 4(b) for the elastically supported one ($C_T = C_R = 10$). The abscissa of each figure denotes the normalized modal displacements $\bar{W}^{(r)}(\tilde{x})$ and the ordinate denotes the axial coordinates with origin located at the lower (larger) end of the tower defined by $\tilde{x} = L_1 - x$, where L_1 is the total length of the complete wedge beam and x is the coordinate with origin at the tip end of the complete wedge beam (cf. Fig. 1). Either in Fig. 4 or Fig. 5, the curves with symbols ○ (or ●), + (or ×), Δ (or ▲), □ (or ■) and ☆ (or ★) denote the 1st, 2nd, 3rd, 4th and 5th mode shapes, respectively. From Figs. 4(a) and (b), one sees that the solid curves and the dashed ones overlap each other. This is as per one's expectation, because the associated natural frequencies obtained from the exact solution and those from the FEM are very close to each other as one may see from Tables 3 and 4. From Fig. 4(b), one sees that the 1st mode vibration is near a rigid-body mode with a combination of sliding

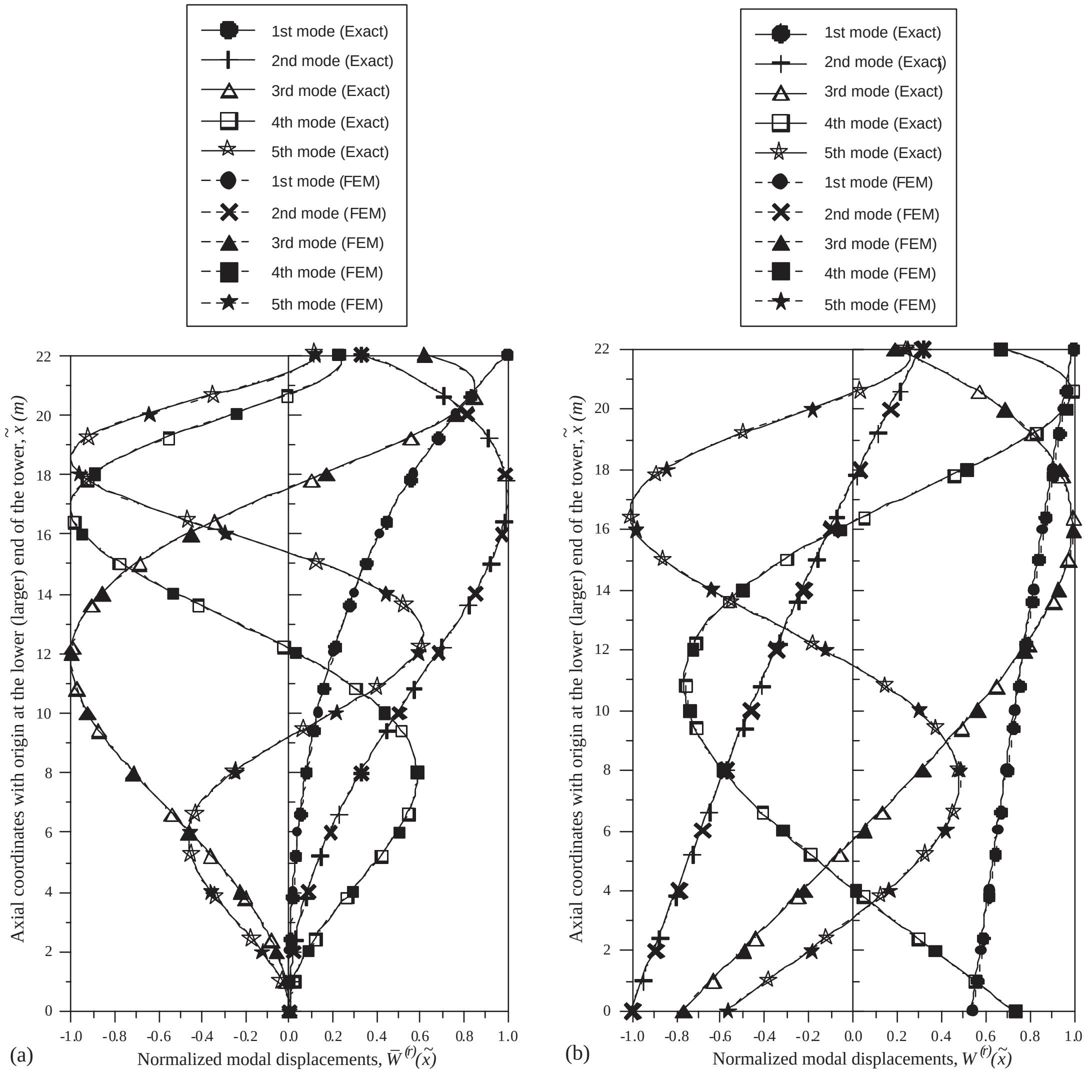

Fig. 4. The lowest five mode shapes of the fully immersed tower ($d = L = 22\,\text{m}$) obtained from exact solutions (———) and from FEM (– – – –): (a) fixed supported ($C_T = C_R = 0$); (b) elastically supported ($C_T = C_R = 10$).

and rocking motions of the elastically supported tower. The 2nd mode shape is similar to the 1st one, but the component due to the elastic deformation is slightly larger.

Fig. 5(a) shows the influence of added mass on the lowest five mode shapes of the fixed supported tower (with $C_T = C_R = 0$) and Fig. 5(b) shows that of the elastically supported one (with $C_T = C_R = 10$) obtained from the exact solutions, in which the solid curves (———) denote the mode shapes of the wet beam (with $d = L = 22\,\text{m}$) and the dashed curves (– – – –) denote those of the dry beam (with $d = 0$). Not much differences between the solid curves and the dashed ones in Fig. 5 reveal that the mode shapes of the wet beam are very close to the corresponding ones of its dry beam.

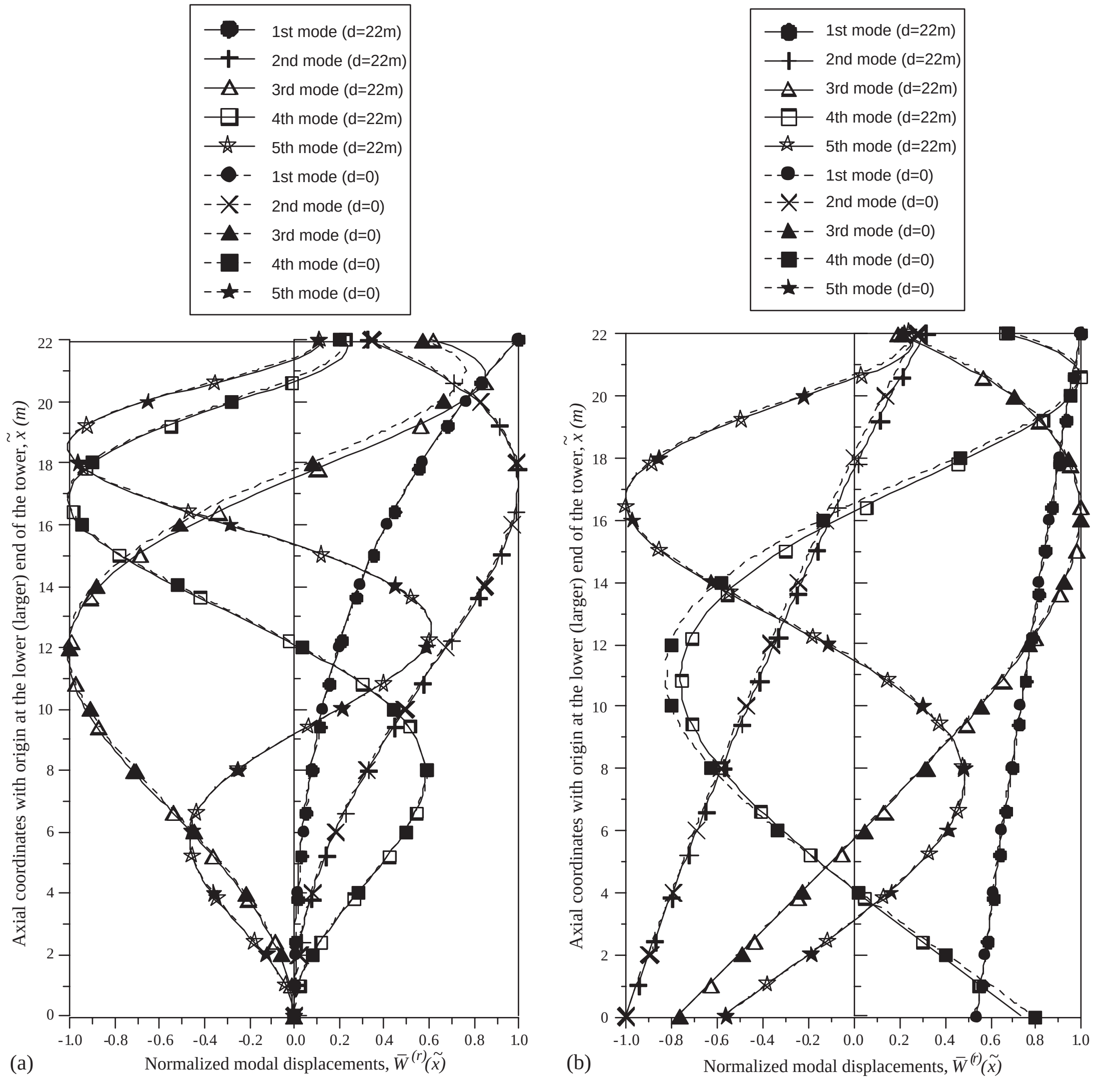

Fig. 5. The lowest five mode shapes of the tower obtained from the exact solutions for (a) fixed supported ($C_T = C_R = 0$) and (b) elastically supported ($C_T = C_R = 10$): ——— for wet modes ($d = L = 22\,\mathrm{m}$); – – – – for dry modes ($d = 0$).

5. Conclusions

1. The exact natural frequencies and the corresponding mode shapes of an immersed doubly tapered beam can be determined using the theory presented in this paper. The reliability of the numerical results has been confirmed by those obtained from the conventional finite element method.
2. For convenience, one may predict the dynamic behaviours of a "fixed" supported tower from those of its corresponding "elastically" supported one by letting the sliding spring constant k_T and the rocking spring constant k_R to approach infinity, e.g., $k_T = k_R = 10^{26}$ N/m (or N m).

3. The influence of water depths (d) on the first natural frequencies ω_1 of a tower is negligible, no matter whether the soil stiffness ratios $C_T = C_R = 0$, 0.1, 1.0 or 10, particularly for the fixed supported tower (with $C_T = C_R = 0$). However, the last phenomenon is not true for the other orders of natural frequencies ω_r ($r = 2 - 5$). For the latter, the influence of water depth on the natural frequencies of a tower increases with the increase in vibration order r.
4. Either fixed or elastically supported, the influence of added mass on the mode shapes of a tower is negligible. In other words, the mode shapes of a wet tower (with $d \neq 0$) are very close to the corresponding ones of the dry tower (with $d = 0$).

References

[1] M. Gürgöze, A note on the vibration of restrained beam and rods with point masses, *Journal of Sound and Vibration* 96 (4) (1984) 467–468.
[2] M. Gürgöze, On the vibrations of restrained beams and rods with heavy masses, *Journal of Sound and Vibration* 100 (4) (1985) 588–589.
[3] P.A.A. Laura, C.P. Filipich, V.H. Cortinez, Vibrations of beams and plates carrying concentrated masses, *Journal of Sound and Vibration* 112 (1987) 177–182.
[4] B. Posiadala, Free vibration of uniform Timoshenko beams with attachments, *Journal of Sound and Vibration* 204 (2) (1997) 359–369.
[5] R.E. Rossi, P.A.A. Laura, D.R. Avalos, H.A. Larrondo, Free vibration of Timoshenko beams carrying elastically mounted concentrated masses, *Journal of Sound and Vibration* 165 (1993) 209–223.
[6] N.G. Stephen, Vibration of a cantilevered beam carrying a tip heavy body by Dunkerley's method, *Journal of Sound and Vibration* 70 (1980) 463–465.
[7] K. Takahashi, Eigenvalue problem of a beam with a mass and spring at the end subject to a force, *Journal of Sound and Vibration* 71 (3) (1980) 453–457.
[8] M.W.D. White, G.R. Heppler, Vibration modes and frequencies of Timoshenko beams with attached rigid bodies, *Journal of Applied Mechanics* 62 (1995) 193–199.
[9] J.S. Wu, T.L. Lin, Free vibration analysis of a uniform cantilever beam with point masses by an analytical-and-numerical-combined method, *Journal of Sound and Vibration* 136 (2) (1990) 201–213.
[10] N.M. Auciello, Transverse vibration of a linearly tapered cantilever beam with tip mass of rotatory inertia and eccentricity, *Journal of Sound and Vibration* 194 (1) (1996) 25–34.
[11] R.P. Goel, Transverse vibration of tapered beams, *Journal of Sound and Vibration* 47 (1) (1976) 1–7.
[12] P.A.A. Laura, R.H. Gutierrez, Vibration of an elastically restrained cantilever beam of varying cross-section with tip mass of finite length, *Journal of Sound and Vibration* 108 (1986) 123–131.
[13] T.W. Lee, Transverse vibrations of a tapered beam carrying a concentrated mass, *Journal of Applied Mechanics* 43 (June 1976) 366–367.
[14] H.H. Mabie, C.B. Rogers, Transverse vibrations of double-tapered beams with end support and with end mass, *Journal of the Acoustical Society of America* 55 (1974) 986–991.
[15] J.H. Lau, Vibration frequencies of tapered bars with end mass, *Journal of Applied Mechanics* 51 (1984) 179–181.
[16] J.S. Wu, D.W. Chen, Bending vibration of wedge beams with any number of point masses, *Journal of Sound and Vibration* 262 (2003) 1073–1090.
[17] J.Y. Chang, W.H. Liu, Some studies on the natural frequencies of immersed restrained column, *Journal of Sound and Vibration* 130 (3) (1989) 516–524.
[18] G.D. Han, J.R. Sahglivi, Dynamic model responses of wave-excited offshore structures, *Journal of Engineering Mechanics* 120 (1994) 893–908.
[19] K. Nagaya, Transient response in flexure to general uni-directional loads of variable cross-section beam with concentrated tip inertias immersed in a fluid, *Journal of Sound and Vibration* 99 (1985) 361–378.
[20] K. Nagaya, Y. Hai, Seismic response of underwater members of variable cross section, *Journal of Sound and Vibration* 103 (1985) 119–138.

[21] A. Uscilowska, J.A. Kolodziej, Free vibration of immersed column carrying a tip mass, *Journal of Sound and Vibration* 216 (1) (1998) 147–157.
[22] J.S. Wu, K.W. Chen, An alternative approach to the structural motion analysis of wedge-beam offshore structures supporting a load, *Ocean Engineering* 30 (14) (2003) 1791–1806.
[23] J.S. Wu, L.K. Chiang, 2004. Free vibrations of solid and hollow wedge beams with rectangular or circular cross sections and carrying any number of point masses,, *International Journal for Numerical Methods in Engineering* 60 (2004) 695–718.
[24] L. Meirovitch, *Analytical Methods in Vibration*, MacMillan, London, 1967.
[25] F.H. Todd, *Ship Hull Vibration*, Edward Arnold, London, 1961.
[26] T. Sarpkaya, Forces on cylinders and spheres in a sinusoidally oscillating fluid, *Journal of Applied Mechanics* E42 (1975) 32–37.
[27] G.N. Watson, *A Treatise on the Theory of Bessel Functions*, Cambridge University Press, Cambridge, 1952.
[28] F.D. Faires, R.L. Burden, *Numerical Methods*, PWS, Boston, 1993.